A sensitive bithiophene-based biosensor for interferon-gamma characterization and analysis

CrossMark

P.I. Tsai [a,1], S.S. Lee [b,1], S.T. Chou [c], C.M. Jan [c], Y.T. Chang [d], A.S.Y. Lee [d], C.K. Lee [a,c,*]

[a] Engineering Science & Ocean Engineering, National Taiwan University, Taipei, Taiwan
[b] Systems Engineering & Naval Architecture, National Taiwan Ocean University, Keelung, Taiwan
[c] Institute of Applied Mechanics, National Taiwan University, Taipei, Taiwan
[d] Department of Chemistry, Tamkang University, New Taipei City, Taiwan

ARTICLE INFO

ABSTRACT

Real-time, label-free monitoring offers a wide range of applications to the biotech field. We developed an integrated bio-sensing platform which adapts a circular polarization interferometry configuration and a phase modulated ellipsometer to improve the performance of biomolecular measurements. An bithiophene-based conductive linker-5′-(mercapto)-[2, 2′-bithiophene]-5-carboxylic acid was developed for detecting antibody–antigen interactions. In this study, the biomarker interferon-gamma (IFN-γ), one of the most important indicators of tuberculosis, was chosen to test and verify the sensitivity of our measurement system. Our experimental results showed that an increase in the concentration of the IFN-γ (64 pM to 1 μM) was usually accompanied by a phase increase. This result is good evidence that our biosensing system can be useful for analyzing biomolecular interactions.

© 2013 Elsevier B.V. All rights reserved.

1. Introduction

With the development of optical and electrochemistry-based bio-metrology techniques, biological determination methods have progressively improved. In recent years, miniaturized devices have advanced quickly to meet the trend towards point-of-care devices. Obtaining biomolecular interactions that are label-free and in real-time is highly sought after.

Optical metrology possesses advantages such as non-invasive probing and label-free detection in biomolecular interaction measurements. Both surface plasmon resonance (SPR) and ellipsometry systems have been previously studied in detail to analyze surfaces with an attempt to measure the phase shift of reflected light beams for wide measurement ranges. As biomolecular detection typically starts out with an assembly of a thin film on a flat substrate, it is particularly suitable for biomolecular ellipsometry measurements. A typical ellipsometer adopts either a rotating-polarizer or a rotating-analyzer configuration to obtain the ellipsometric parameters which generally takes time to obtain and cannot be measured in real-time. Chao and Han installed an ellipsometer equipped with a photoelastic modulator to measure the Ψ and Δ ellipsometric parameters [1]. Although the measurement was in real-time, it still required time for the modulation

of the phase retardation due to the control of the photoelastic modulator. The works published in 2009 by Han et al. [2] detail an ellipsometer configuration with a polarizer azimuth angle set at 45° while recording the sampling beam intensity respectively when the analyzer was rotated to 0°, 60°, and 120° azimuth angles respectively. The parameters Δ and Ψ were calculated by using simple equations in the configuration. We chose three specific rotating angles of the analyzer (e.g. splitting the beam into three and then analyzed them using the three rotated angle analyzers) so that the parameters Δ and Ψ could be calculated easily. Han et al. [3] further demonstrated in 2011 that obtaining an ellipsometric parameter Δ in real-time can provide enough information to analyze the sample variation in situ. The physical meaning of Δ is the phase difference between the p-polarized and s-polarized incident beams. It is similar to the phase difference acquired by a common path phase-shift interferometry technique. The sensitivity enhancement can be attributed to a physical transduction mechanism and to the system configuration [4]. Conceptually, the common-path configuration provides a reference beam denoted by s-polarization for retrieving the exact phase of p-polarized light and which enhances the relative phase difference detection precision [5,6]. For point-wise measurements, phase-interrogation has advantages such as optimal sensitivity, long-term stability, and high resolution. All of this makes it suitable for measuring real-time changes in label-free molecular binding processes [7].

Interferon-gamma (IFN-γ) is a type of endogenously cytokine that is secreted in human peripheral blood lymphocytes [8]. Typically, this biomarker can measure whether a person is at risk for tuberculosis and to indicate the existence of an inflammation [9–11]. SPR technology and electrochemical immunosensors have been used to monitor the

* Corresponding author at: Institute of Applied Mechanics, National Taiwan University, Taipei, Taiwan. Tel.: +886 2 3366 5645; fax: +886 2 3366 5654.
E-mail address: cklee@ntumems.net (C.K. Lee).
[1] These two authors contributed equally to this work.

equilibrium and kinetic constants for neutralizing anti-IFN-γ monoclonal antibodies or IFN-γ binding reactions [12–15]. In recent years, RNA and DNA aptamers have been used to detect IFN-γ using SPR, electrochemical impedance spectroscopy, and quartz crystal microbalance [16–19]. The results show that the detection limit of IFN-γ is 100 fM with the RNA aptamer and 1 pM with the DNA aptamer [16].

Previously, we constructed a system to monitor real-time biomolecular interaction using a common-path configuration sensor [20]. It included a light source, a SPR coupler, a flexible and precise incident angle varying system, as well as a quadrature interferometer detection configuration. One configuration of this system is an ellipsometer. No matter whether it acts as a SPR or as an ellipsometer, the sensitivity of the system depends on accurately controlling the incidence angle of the probing light beam [21]. Since an ellipsometric system is an optical technique that can be used to analyze surfaces, different reactions associated with biomolecular recognition leads to changes in film thickness. More specifically, different molecular bindings can result in different optical phase constants that can be detected by an ellipsometer since it can measure the phase of reflected light and provide a larger measurement range. The aim of this work was to demonstrate the usefulness of a synthesized conductive linker CS20S (5′-(mercapto)-[2, 2′-bithiophene]-5-carboxylic acid) and to detect the concentration difference of IFN-γ by measuring the phase change in corresponding refractive indices. Using the synthesized conductive linker to form the self-assembled monolayer (SAM) on the gold chip surface, it acts as a platform to characterize the biochip surfaces by adopting ellipsometry, SPR signal changes and electrochemical impedance spectroscopy techniques. The main emphasis of this paper is on the applicability of integrating this conductive linker into an ellipsometer which we had previously incorporated into a previous developed system [20]. It is expected that the structural features of the CS20S-modified film surface will be suitable for inhomogeneous solid thin films with respect to the transport of electro-active species.

2. Experimental set-up

2.1. Linker and materials

The conductive linker CS20S, 5′-(mercapto)-[2, 2′-bithiophene]-5-carboxylic acid was synthesized by our team and dissolved in tetrahydrofuran (THF). The reaction formula of the CS20S molecular synthesis is detailed below:

a. n-BuLi (7.5 mmol) was added in drops to a stirred solution of the corresponding 2,2′-bithiophene (5.0 mmol) in anhydrous THF (25 mL) under N_2 at −78 °C. Ethyl chloroformate (5.0 mmol) was added after one hour and the reaction was left to reach ambient temperature gradually, and then extracted with ethyl acetate/H_2O. After removal of the solvent by reducing the pressure, the reaction mixture was purified using chromatography.
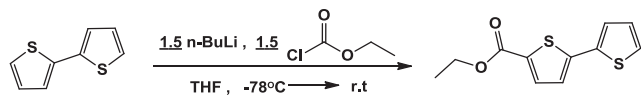
b. Lithium diisopropylamide (6.0 mmol) was added drop by drop to a stirred solution of the corresponding substrate (5.0 mmol) in anhydrous THF (25 mL) under N_2 at −78 °C. Sulfur powder (5.0 mmol) and ethyl chloroformate (5.0 mmol) were added after one hour then left to reach ambient temperature, after which it was then extracted with ethyl acetate/H_2O. The solvent was removed using pressure, and the reaction mixture was purified using chromatography.
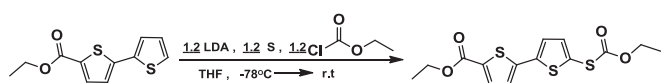
c. Sodium hydroxide (3.0 mmol) was added to a stirred solution of the corresponding substrate (5.0 mmol) in anhydrous THF (25 mL) under N_2 at room temperature for six hours. The reaction was quenched with hydrochloric acid. The crude reaction mixture was extracted with ethyl acetate/H_2O, the solvent removed by pressure and the reaction mixture purified by chromatography.
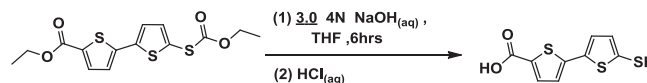
The recombinant human IFN-γ (carrier-free protein), anti-human IFN-γ Ab (monoclonal mouse IgG_{2A}) and mouse IgG_{2A} isotype control (monoclonal mouse IgG_{2A}) were obtained from R&D Systems (Minneapolis, MN, USA). The phosphate-buffered solution (PBS), EDC (N-(3-dimethylaminopropyl)-N′-ethylcarbodiimide hydrochloride), NHS (N-hydroxysuccinimide) and Ethanolamine hydrochloric acid (ETA-HCl) were all obtained from Sigma-Aldrich (St. Louis, MO, USA).

2.2. Assembly of conductive linker on gold chip

A 1 nm Cr layer was deposited between the SF2 (refractive index: 1.64379 at 632.8 nm wavelength, Schott Inc., Duryea, PA, USA) substrate and a 50 nm Au thin film served as the intermediate layer for the bio-chip (Fig. 1(a)). The IFN-γ sensor was fabricated using this gold-coated bio-chip. The chips were cleaned in a detergent solution, then thoroughly ultrasonically cleaned with distilled H_2O and dried with nitrogen. The cleaned chip was then immersed in 5 mM CS20S solution for 12 h to modify the chip surface. Finally, the chips were rinsed with a THF solution, ethanol, and distilled H_2O. The SAM derived from the developed constructive linker on the gold chip surface was characterized by the SPR and ellipsometry signal changes.

2.3. SPR and ellipsometry systems

In our measurement system, a circularly polarized ellipsometer was integrated with a quadrature interferometer (Fig. 1(b)) [22]. The light source used was a 635 nm wavelength laser diode module (VHK™ Circular Beam Visible Laser Module, Edmund Optics Inc.) and driven by a 5 V DC power supply. Two incident light beams (p- and s-polarized) were adopted as the monochromatic light source propagating along a common path. The integrated miniaturized system named OBMorph (also known as Opto-Bio Morphin) adopted four photo-detectors to perform the differential phase measurement [20,21]. The sensitivity for the phase detection in the system was previously experimentally verified to be 8.2×10^{-6} (1/RIU). A FTA (fault tolerance algorithm) was integrated in the OBMorph System to compensate and to increase the system measurement reliability. By simulating the reflectivity and reflected phase of the SPR response, an estimated change of the p-polarized light was found to be within the linear region when the 50 nm Au/1 nm Cr was deposited on top of the SF2 substrate refractive index illuminated by a 635 nm wavelength incident light beam. (Fig. 1).

2.4. Analysis of CS20S assembly and IFN-γ binding

Experimental work was performed using the OBMorph platform [20,21]. The flow rate was set at 30 μL/min. A PBS buffer (10 mM PBS, 100 mM NaCl, 2 mM KCl, pH 7.4) was injected into the OBMorph to cleanse the prepared surface. The linker on the chip surface was activated with a 1:1 mixture of 0.4 M EDC and 0.1 M NHS for 10 min. For the mouse monoclonal anti-human IFN-γ Ab and IgG_{2A} immobilization, the antibodies were warmed to room temperature, and then dissolved in a PBS buffer in a 0.5 μM concentration. The antibody solution was injected and was allowed to interact with the linker for 20 min. 1 M ETA-HCl blocking solution (pH 8.5) was injected to reduce non-specific
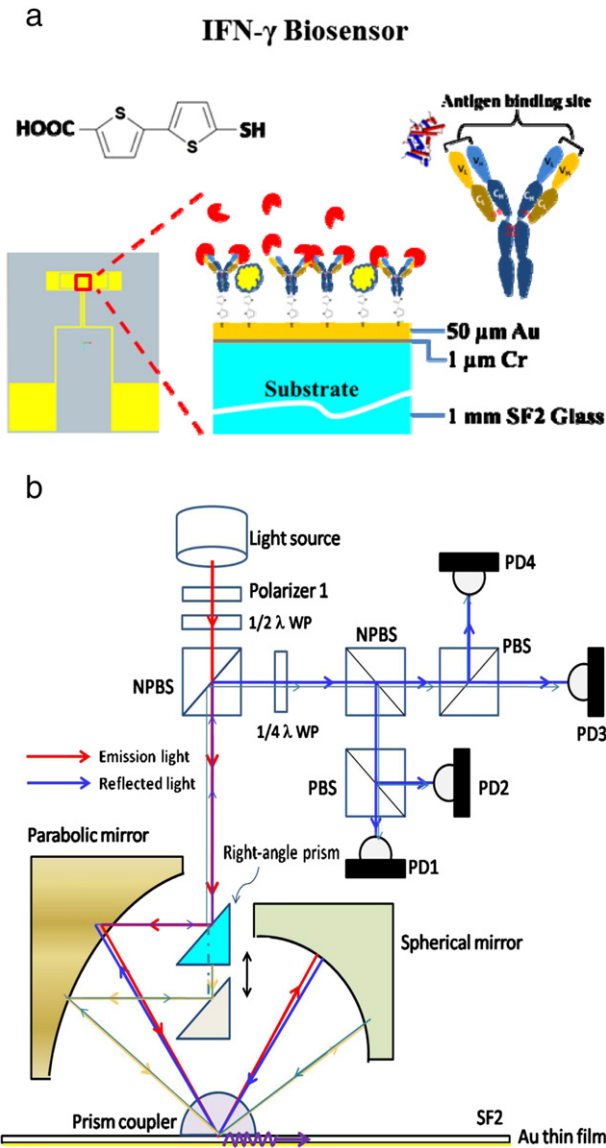
Fig. 1. (a) Fabrication of an IFN-γ biosensor. (b) Schematic of an OBMorph system.

interference and to obtain an accurate signal. The IFN-γ was dissolved in the PBS buffer and then introduced into the OBMorph at various concentrations. After each measured IFN-γ concentration, the chip was washed with the PBS buffer.

3. Results and discussions

Fig. 2 illustrates the simulation results (Film Wizard Software, v.9.0.4). These simulation results were obtained from illuminating a 635 nm wavelength light beam onto a SF2 substrate coated with 50 nm Au and 1 nm Cr. A phase difference between the *p*- and *s*-polarized reflected light beams was compared to the simulated sample refractive indices at different incident angles (Fig. 2(a)). The reflected optical phases of the *p*- and *s*-polarizations at different incident angles are shown in Fig. 2(b). Results show an unequal phase-difference dependency on the *p*- and *s*-polarization waves at various incident angles. Fig. 3 shows the inclined Lissajous curve induced by the incorrect orientation of the quarter-wavelength plate due to misalignment. A signal processing algorithm called fault tolerance algorithm (FTA) [21–24] was performed to show the optimal mapping data with a least-square solution using an iteration algorithm, $P \equiv 2r_p^2 r_s^2 \cos 2\Delta = I_2 - I_4$ and $Q \equiv 2r_p^2 r_s^2 \sin 2\Delta = I_1 - I_3$. A LabVIEW program was used to adjust the experimental intensity levels

detected by the photodetectors. We used different concentrations of a glucose solution to verify the bio-chip platform measurement accuracy.

Fig. 4 shows a nearly linear relationship between the phase measured by OBMorph and the concentration of the glucose solution. The obtained coefficient of determination R^2 of the trend line was 0.9950. The refractive indices at different concentrations of the glucose solution were obtained using a commercially available refractive index meter (Kyoto Electronics Manufacturing Co., RA-130). Taking the range of the ellipsometry measurements into account, the incidence angle was set at 64.1141°.

We evaluated the accuracy of the OBMorph platform, and show some results of a variation characterized by the measured variances in concentration and chips. For an analysis of the CS20S assembly and IFN-γ binding, CS20S molecules were thiolated to ensure the self-assembly on the gold chips. The assembly of the CS20S molecules, anti-human IFN-γ Ab and binding of IFN-γ was investigated. Unmodified chips and non-conjugated antibodies were tested to verify the attachment of the specific binding to the antibody. Figs. 5 and 6 show the rapid binding of the biomolecules onto the gold surface. Once the antibody was bound onto the chip, subsequent injection of the ETA and a related sensing layer were used at varying concentrations (64 pM–1 μM, 5-fold serial dilutions) of human recombinant IFN-γ on the same chip to show additional phase signal increases. The experimental process was set up with continuous detection at different concentrations of IFN-γ injected into the same chip by a single cycle. In Fig. 5(a), the phase variation in real-time indicates the immediately
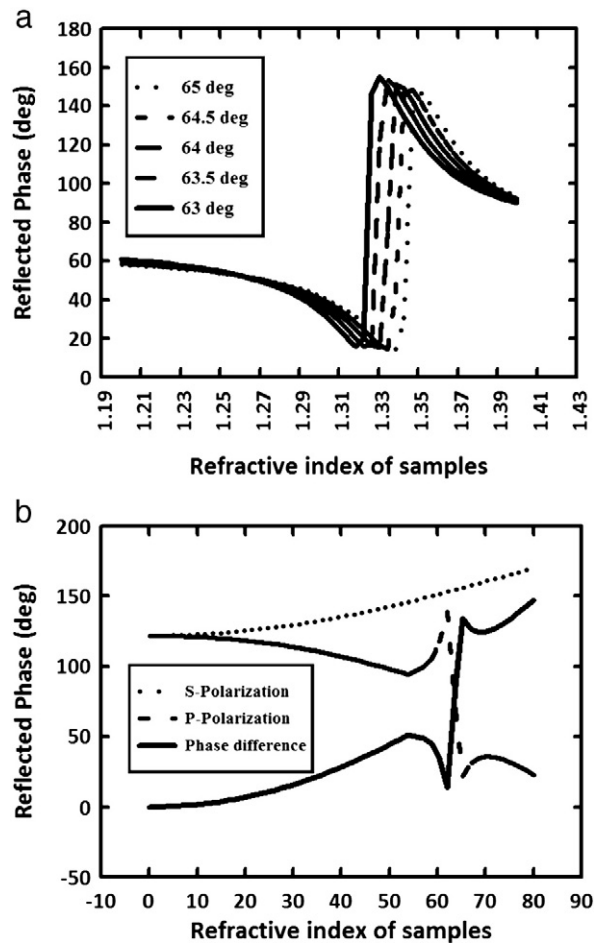

Fig. 2. Simulation results of SPR *p*- and *s*-polarized phase detection obtained from illuminating a 635 nm wavelength light beam onto a SF2 substrate coated with 50 nm Au and 1 nm Cr. (a) Phase difference of *p*- and *s*-polarized reflected light beam compared to sample refractive indices at different incident angles. (b) Reflected optical phase of *p*- and *s*-polarizations and the phase difference at different incident angles.
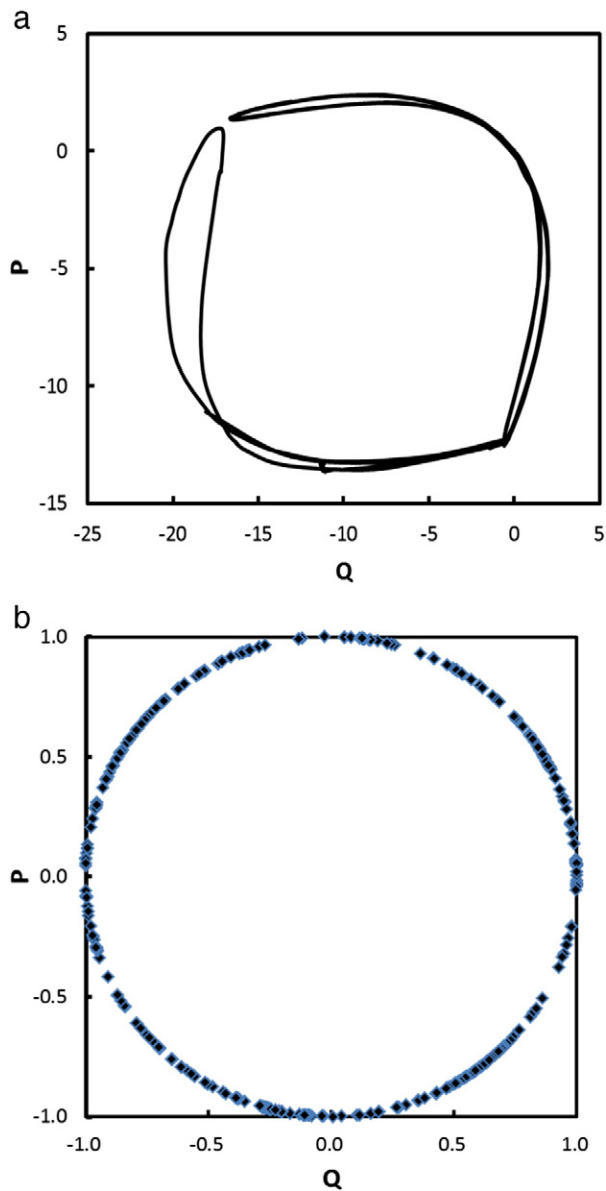
Fig. 3. Experimental response of Lissajous curve. (a) Before FTA calibration and (b) After FTA calibration.
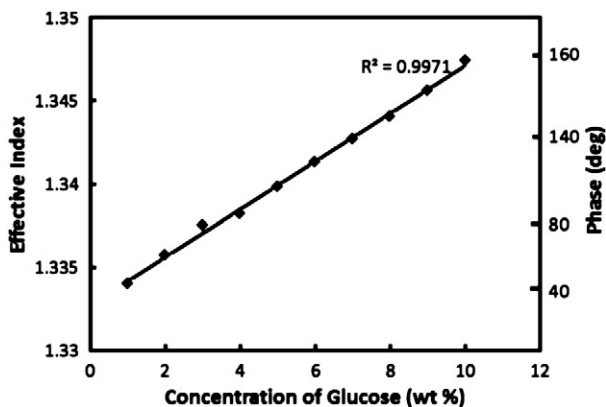

Fig. 4. Experimental results of the effective index and phase difference at various glucose concentrations.

activation process of EDC/NHS, a full immobilization of an anti IFN-γ antibody which is a non-specific type blocking with ETA. The IFN-γ affinity interactions at 0.5 μM and 1 μM concentrations were also observed after the saturation binding of the analyte. In summary, we used monoclonal anti-human IFN-γ Ab to recognize recombinant human IFN-γ (carrier-free protein). In addition, the IFN-γ reagent was chosen with a carrier-free condition recognized by the anti-human IFN-γ Ab as a positive control in our system.

From an immunology perspective, we compared the two antibodies, mouse IgG$_{2A}$ isotype control and anti-human IFN-γ Ab, to check whether the antibodies caused non-specific binding of IFN-γ protein on this platform. Full trace of the analyte isotype control data is shown in Fig. 5(b). A nonspecific mouse IgG$_{2A}$ isotype control instead of the anti-human IFN-γ Ab was dissolved in the PBS with IFN-γ in an identical experiment. The same concentration of IFN-γ protein was injected onto the chip with IgG$_{2A}$ immobilization. Initial analysis of IFN-γ found it was not possible to bind to the IgG$_{2A}$ at a level from 1.6 nM to 40 nM. The data shows that at 1.6 nM, 8 nM and 40 nM negative fractions, our set-up provided us with a way to obtain 0.5 μM at 10.2516 phase degree (vs. 57.5665° positive), and 1 μM at 12.1351 phase degree (vs. 92.1565° positive). The results indicated that a signal associated with IFN-γ protein shows up clearly at a high background signal from high concentrations of nonspecific mouse IgG$_{2A}$ isotype control. In other words, isotype control related to non-specific binding will not interfere with the true signal of interest. Since the background signal is associated the immobilization of a high concentration of antibodies, our data set demonstrates that the measurement of IFN-γ shows an effective selection in the values of positive control. The results clearly show that our configuration used with the conductive linker CS20S can detect different concentrations of IFN-γ which confirms our system sensitivity.

The total phase changes with the concentration variation depended on the incidence angle setting. The incident angle was near the SPR angle, and data shows that the total phase change increases under the
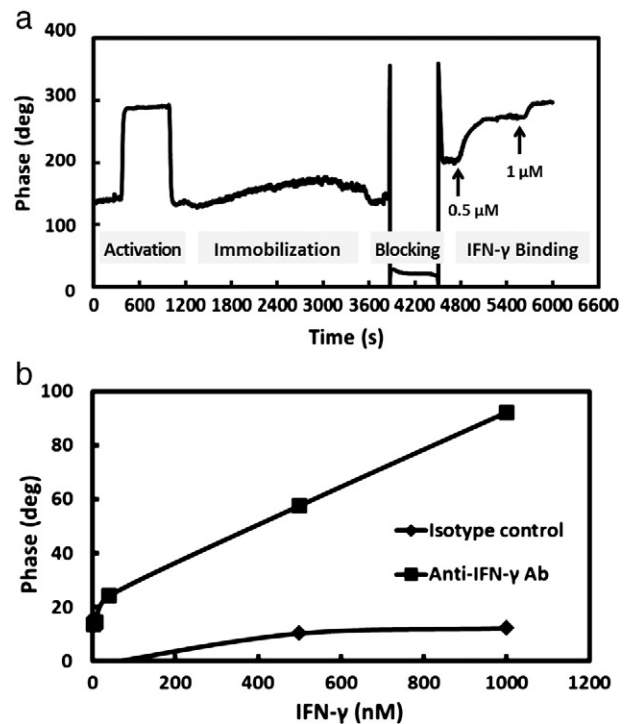

Fig. 5. A real-time measurement of a bithiophene-based biosensor. (a) Phase changes induced by biomolecular interaction measured in continuous real-time during binding process of linker activation, antibody immobilization at 0.5 μM and 1 μM of IFN-γ obtained at a steady state. (b) Specific binding of IFN-γ protein with anti-IFN-γ Ab as a positive control and non-specific binding with IgG$_{2A}$ isotype control.
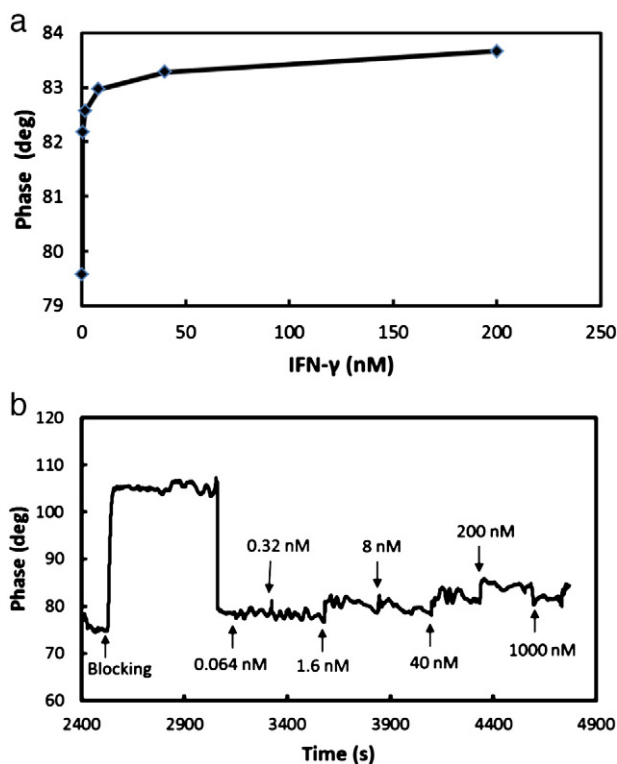
Fig. 6. Experimental results of a phase difference at various concentrations of INF-γ: (a) Phase change at varying concentrations. (b) Real-time phase change at varying concentrations.

same concentration difference. Fig. 6 shows representative phase signals at different IFN-γ concentrations binding to the antibody layer. Fig. 6(a) shows that phase increased with increased IFN-γ concentration in an almost linear relationship. The phase changes were between 79.5696 and 83.6599° whereas a direct steep linear relationship would have been from 82.175 to 82.9647° and the IFN-γ concentrations from 0.32 nM to 8 nM. There was a small signficant linear relationship between the phase difference and concentration variation from 8 nM to 200 nM. In contrast to Fig. 5 which shows between 203.0135 and 295.3298° at 0.5 μM and 1 μM concentrations, the experimental data in Fig. 6 shows that the phase measuring mode displays a higher sensitivity within the system.

We evaluated the accuracy of OBMorph, and show some of the results of the variation characterized by the measured variances of concentrations and chips. To assess the linearity of the assay, samples were spiked with high concentrations of IFN-γ in various microtubes and diluted with a PBS buffer to produce samples with values within the dynamic range of the assay. More than seven samples of known concentrations were tested on one chip (Figs. 6(a) and 6(b)) to assess the intra-assay precision. To assess the intra-assay precision in Fig. 6, we found that the maximum background noise was a 0.596° phase which corresponded to a 0.33% background noise signal before any sample was added to the chip. After a sample with 40 nM concentration was added to the chip, the measured phase angle was found to be 21.19°. The phase angle was measured 100 times at this state and the standard deviation of the signal measured was 1.284°, which corresponded to a concentration error of 2.42 nM. More specifically, the intra-assay error of our system is around 6%. For an inter-assay error estimation, a 21.27° phase angle change was obtained when a 1000 nM concentration sample was added. The standard variation of the experimental phase signal obtained across 3 chips was found to be 3.47°, which equaled to a 13.21% sample concentration error. That is, the inter-assay error of our system is around 13.21%. It is clear that the inter-assay

precision is lower than that of the intra-assay. This is not surprising as different chips create additional errors. We traced the additional errors to the base-plane design between the optical metrology sub-system of the OBMorph and the biochip. Some additional measures to improve this design are currently underway. In this study, we present an intra-chip variability and inter-chip variability. It should be noted that it is important to consider the incident angle dependence by which the amount of inter-chip variation is affected. The biomolecular interaction changes were discriminating at the lower concentrations, as even the incident angles were not close to the SPR angle and the phase changes were not obvious. Under optimal conditions, the detection limit in our system probability was identified to be better than 64 pM [22]. We found that the sensitivity of the phase-interrogation SPR was predominantly influenced by the optimization of the sample incidence angles.

4. Conclusions

Our developed metrology platform includes biological measurement data based on interrogating angular and phase functions from SPR and ellipsometry. Our experimental results clearly show that higher sensitivity and higher resolution can be obtained by adopting our developed bithiophene-based conductive linker. The performance verification results of this system demonstrate the suitability and accuracy of the selected biomarker in our optical system. The advantages of this label-free and real-time monitoring system can be used to analyze biological reactions such as thickness of thin film layers. Furthermore, it provides us with a good tool to measure protein–protein interaction processes in biosensing applications.

Acknowledgments

References

[1] Y. Chao, C. Han, Sensors Actuators B Chem. 121 (2) (2007) 490.
[2] C.Y. Han, Z.Y. Lee, Y.F. Chao, Appl. Opt. 48 (17) (2009) 3139.
[3] C.Y. Han, C.W. Lai, Y.F. Chao, K.C. Leou, T.L. Lin, Appl. Surf. Sci. 257 (7) (2011) 2536.
[4] A. Shalabney, I. Abdulhalim, Laser Photonics Rev. 5 (4) (2011) 571.
[5] P.P. Markowicz, W.C. Law, A. Baev, P.N. Prasad, S. Patskovsky, A.V. Kabashin, Opt. Express 15/4 (2007) 1745.
[6] T. Nakata, M. Watanabe, Opt. Rev. 15 (6) (2008) 276.
[7] Y.D. Su, S.J. Chen, T.L. Yeh, Opt. Lett. 30 (12) (2005) 1488.
[8] H.C. Kelker, J. Le, B.Y. Rubin, Y.K. Yip, C. Nagler, J. Vilcek, J. Biol. Chem. 259/7 (1984) 4301.
[9] J.L. Flynn, J. Chan, K.J. Triebold, D.K. Dalton, T.A. Stewart, B.R. Bloom, J. Exp. Med. 178 (6) (1993) 2249.
[10] M. Zhang, Y.G. Lin, D.V. Iyer, J.H. Gong, J.S. Abrams, P.F. Barnes, Infect. Immun. 63 (8) (1995) 3231.
[11] A. Verbon, N. Juffermans, S.J. Van Deventer, P. Speelman, H. Van Deutekom, T. Van Der Poll, Clin. Exp. Immunol. 115/1 (1999) 110.
[12] N. Ruegg, G. Williams, A. Birch, J.A. Robinson, D. Schlatter, W. Huber, J. Immunol. Methods 183 (1995) 95.
[13] M. Dijksma, B. Kamp, J.C. Hoogvliet, B.W.P. van, Anal. Chem. 73 (2001) 901.
[14] G. Stybayeva, M. Kairova, E. Ramanculov, A.L. Simonian, A. Revzin, Colloids Surf. B: Biointerfaces 80 (2) (2010) 251.
[15] N. Tuleuova, C.N. Jones, J. Yan, E. Ramanculov, Y. Yokobayashi, A. Revzin, Anal. Chem. 82 (2010) 1851.
[16] K. Min, M. Cho, S.Y. Han, Y.B. Shim, J. Ku, C. Ban, Biosens. Bioelectron. 23 (2008) 1819.
[17] C.C. Chang, S. Lin, C.H. Lee, T.L. Chuang, P.R. Hsueh, H.C. Lai, C.W. Lin, Biosens. Bioelectron. 37 (1) (2012) 68.
[18] J. Zhao, C. Chen, L. Zhang, J. Jiang, R. Yu, Biosens. Bioelectron. 36 (2012) 129.
[19] H.H. Jeong, N. Erdene, J.H. Park, D.H. Jeong, H.Y. Lee, S.K. Lee, Biosens. Bioelectron. 39 (2013) 346.
[20] W.L. Hsu, S.S. Lee, C.K. Lee, J. Biomed. Opt. 14/2 (2009) 024036.
[21] C.M. Jan, Y.H. Lee, K.C. Wu, C.K. Lee, Opt. Express 19/6 (2011) 5431.
[22] C.M. Jan, Y.H. Lee, C.K. Lee, in: T. Vo-Dinh, J.R. Lakowicz (Eds.), Proc. of SPIE, vol. 7577, 2010, p. 12.
[23] W.J. Wu, C.K. Lee, C.T. Hsieh, Jpn. J. Appl. Phys. 38 (1999) 1725.
[24] C.K. Lee, G.Y. Wu, C.T. Teng, W.J. Wu, C.T. Lin, W.H. Hsiao, H.C. Shih, J.S. Wang, S.C. Lin, C.C. Lin, C.F. Lee, Y.C. Lin, Jpn. J. Appl. Phys. 38 (1999) 1730.